Received: 17 February 2020 | Revised: 25 February 2020 | Accepted: 27 February 2020

DOI: 10.1002/jsid.880

SPECIAL SECTION PAPER

WILEY

Increasing the pixel density for VR displays with a polarization grating

Junyu Zou | **Tao Zhan SID Student Member** | **Jianghao Xiong SID Student Member** | **Shin-Tson Wu SID Fellow**

College of Optics and Photonics, University of Central Florida, Orlando, Florida

Correspondence
Shin-Tson Wu, College of Optics and Photonics, University of Central Florida, Orlando, FL 32816.
Email: swu@creol.ucf.edu

Funding information
GoerTek Electronics; Intel Corporation

Abstract

An optical approach to increase the pixel density by using a Pancharatnam-Berry deflector (PBD), which generates two virtual shifted-pixel grids based on polarization multiplexing, is demonstrated. A three-layer multi-twist PBD is fabricated, which can achieve high diffraction efficiency, broad bandwidth, and large incident angle in the visible spectral region.

KEYWORDS

broadband and wide-view, liquid-crystal devices, multiplexing, PBD, resolution enhancement

1 | INTRODUCTION

Polarization grating (PG) is a device that modulates the polarization state of the incident light in one direction, and it can angularly separate the incident light into two output waves with orthogonal polarization states.[1, 2] Right-handed circularly polarized (RCP) light and left-handed circularly polarized (LCP) light are adopted as polarization eigenstates in a PG if it is fabricated by polarization holography, which is based on continuous Pancharatnam-Berry (PB) phase changing in one dimension.[3–6] PB phase PG or deflector (PBD) can achieve polarization selectivity with high efficiency and compact size so that these devices attract great attention in recent years, and one important application of PBD is to enhance the resolution in head-mounted displays.[7, 8]

At present, most of commercial virtual reality (VR) products have a field of view (FOV) around 100° and ~6 arcmin of angular resolution, but human eyes can resolve 1 arcmin. When the display resolution is not high enough, the screen-door effect caused by the black matrices will appear. To solve this problem, high-resolution display panels with sufficient pixels per inch (PPI) is required. Currently, over 1000 PPI display panels have been reported,[9] which can reach half requirement of the human eye acuity. However, challenges like decreased display luminance and large data flow rate still exist, especially as the pixel density increases.

Recently, two approaches have been proposed to solve the low-resolution problem in head-mounted displays: foveated displays[10] and shifted superimposition method.

Foveated displays make use of the characteristic of human eye acuity, which is the highest in the fovea region and decreases significantly as the eccentric angle increases.[11] Therefore, high resolution in the whole FOV is not necessary but only for the fovea region. Foveated display is the one trying to match the human eye acuity, ie, high resolution in the fovea region and decreased resolution in the peripheral area, as Figure 1 depicts. In this way, the total number of pixels can be significantly reduced while preserving high-resolution experience. However, the position of fovea region would shift with eye movement, so that foveated displays need extra eye-tracking and beam steering system in the headset.[12] On the other hand, the human eye acuity decreases continuously as the eccentric angle increases, but the foveated displays show abrupt change of pixel density between fovea region and peripheral area. Gradual imaging blur should occur near the edge pixels of the fovea region in order to obtain smooth resolution change.

The other approach is superimposing spatially displaced pixel grids to achieve higher resolution. The

 © 2020 Society for Information Display

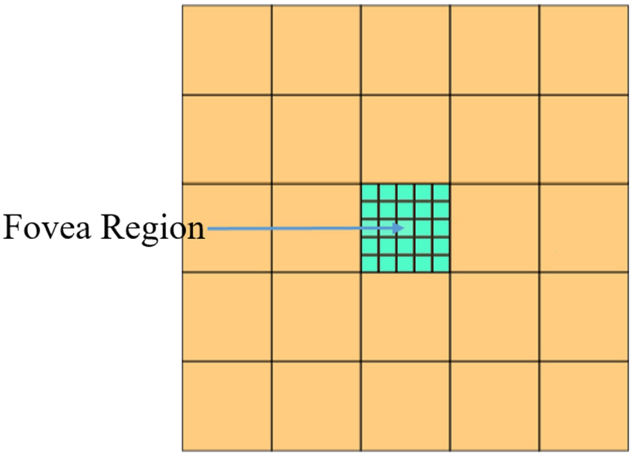

FIGURE 1 High resolution (cyan) and low resolution (orange) areas of foveated display

operation principle is shown in Figure 2. An early method to generate spatially displaced pixel grids is based on mechanical image shifter.[13] The original image and shifted image are present alternately in time domain. Because the time gap between frames is very short, the observer would see original image and shifted image overlapping in space. With carefully designed shifting distance and direction, high-resolution image that has doubled PPI can be achieved. The trade-off of this approach is twofold: mechanical vibration and framerate reduction. Although an electro-optic image shifter can replace the mechanical image shifter to avoid mechanical vibration,[9] the framerate reduction still remains unsolved. If cascading one more display,[14] the framerate can be maintained, but the trade-off is lower optical efficiency.

In this paper, an optical approach based on polarization multiplexing[15] is demonstrated to improve the resolution for VR displays without losing framerate and optical efficiency. A high-efficiency broadband and wide-view PBD is also fabricated.

2 | OPERATION PRINCIPLES

2.1 | Resolution-enhanced near-eye display system

The operation principle of our approach is to optically separate each display pixel into two virtual pixels and superimpose them to get higher pixel density, as Figure 3A illustrates. The difference between our design and the previous shifted superimposition methods is that we present the two virtual panels simultaneously, and the original panel is not observable. In this way, same performance as Figure 2B shows can be achieved without the penalty of framerate reduction. The proposed display system is shown in Figure 3B. In comparison with traditional VR system, a PBD and the polarization modulation layer (PML), which consists of a pixelated polarization rotator (PPR) and a quarter-wave plate (QWP), is added after the eyepiece lens and display panel, respectively.

PBD is a critical component to achieve pixel separation, because it is a PG and it has high diffraction efficiency in the $\pm$1st orders, which means that the zero order (origin pixel) is negligible. For near-eye displays, the direction of output beams corresponds to the pixel locations on the display penal, as Figure 3B depicts. By separating one beam to two first-order beams with different directions, the PBD accomplishes the function for doubling the number of pixels. The grating period and the focal length of eyepiece lens are adjusted so that the diagonal shifting length from original pixel to virtual pixels is $\left(\sqrt{2}/4\right)P$, where P is the display panel pixel pitch, and a new pixel grid with half pixel pitch can be generated. Although some parts of the edge pixels are not overlapped, when the number of pixels is very large, the influence of the edge pixels is negligible.

In order to achieve the desired high-resolution image, we need not only diagonally shift the original pixels to

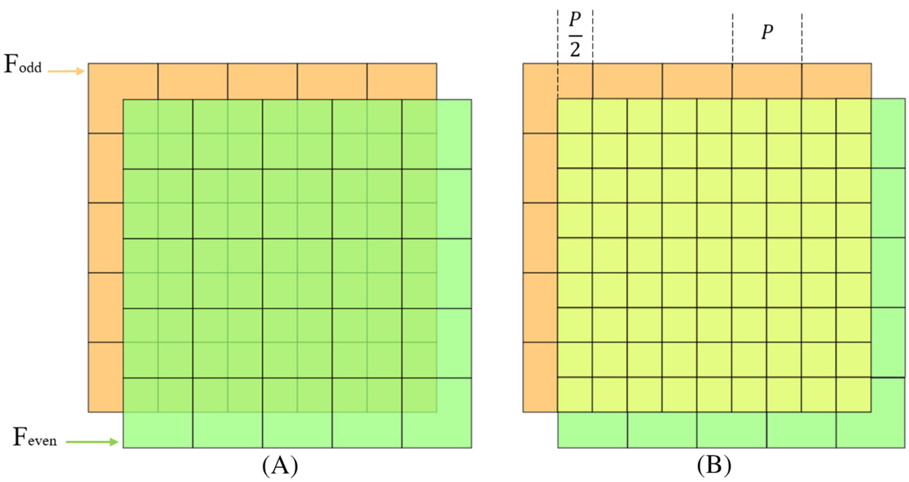

FIGURE 2 Operation principle of the shifted superimposition method to improve the resolution density. (A) The original panel (orange) presents at odd frames (F_{odd}), and the shifted panel (green) presents at even frames (F_{even}). (B) A new pixel grid (yellow) with half a pixel pitch (P/2) is formed by superimposing two panels

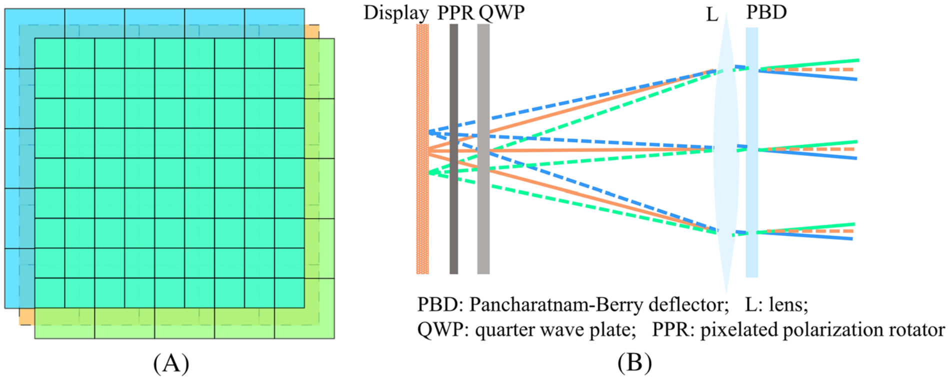

FIGURE 3 (A) The original panel (orange) is separated into two virtual panels (blue and green); the new half pixel pitch grid (cyan) is formed by superimposing two virtual panels. (B) Schematic illustration of the resolution-enhanced near-eye display system based on polarization multiplexing

two opposite directions with certain distance but also adjust the ratio of brightness separation between two correlated virtual pixels. If the original image pixel number is N, then the desired high-resolution image should have $4N$ pixels, and the degree of freedom is $4N$. By adjusting the brightness separation ratio between two virtual pixels, the brightness of each pair of pixels in the two low-resolution virtual images can be controlled independently so that the degree of freedom can be modulated is $2N$. Therefore, this is an overdetermined problem with $4N$ constraints and $2N$ variables, whose optimal solution can be found by solving following minimum loss function:

$$\arg\min_{V} \| M_{4N\times 2N} V_{2N\times 1} - T_{4N\times 1} \|^2, V_{2N\times 1} = \begin{bmatrix} V_1 \\ V_2 \end{bmatrix}, \quad (1)$$

where T contains the pixel values of the desired high-resolution image, M is the mapping matrix between high-resolution image contents and the two virtual images (V_1 and V_2). The product of MV is generated resolution-enhanced image. An example of the mapping procedure is illustrated in Figure 4. The 11th pixel in the desired high-resolution image consists of first and seventh pixels in two virtual panels. Thus, the 11th row of mapping matrix M, which corresponding to the 11th pixel in the high-resolution image, are zeros except for the first

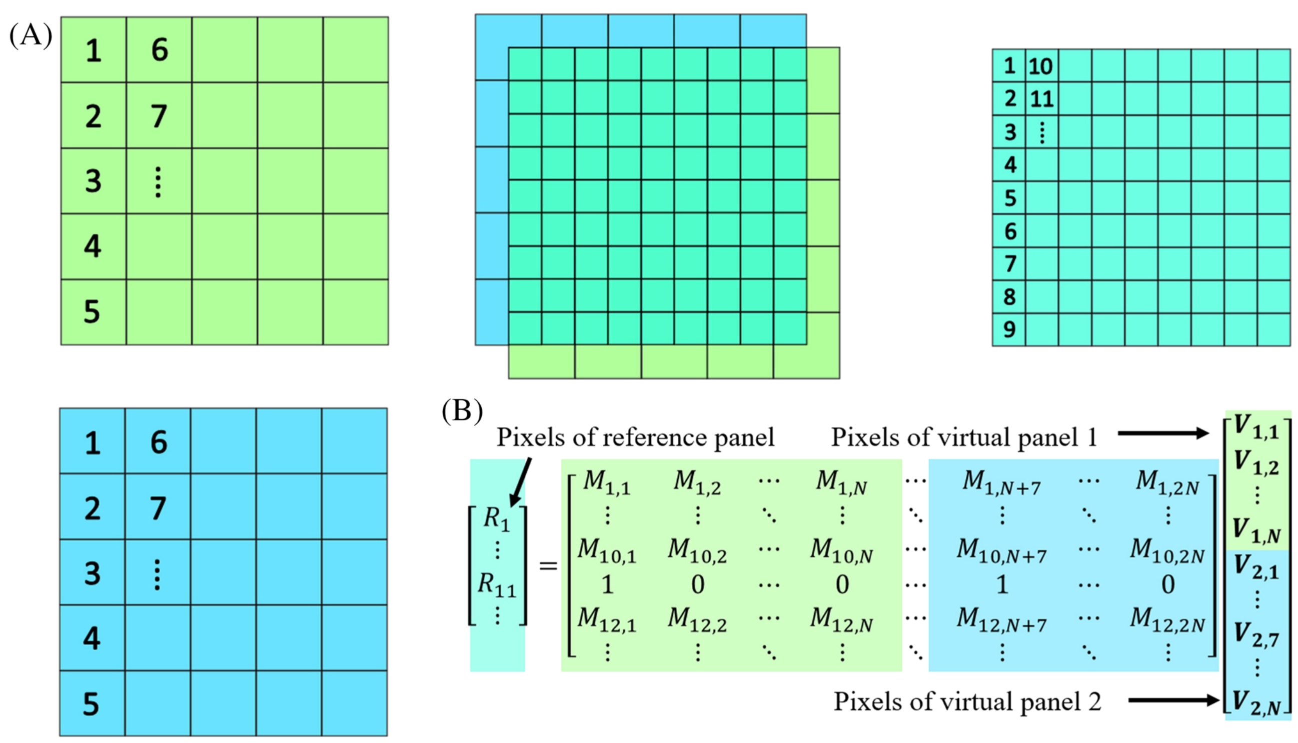

$$\begin{bmatrix} R_1 \\ \vdots \\ R_{11} \\ \vdots \end{bmatrix} = \begin{bmatrix} M_{1,1} & M_{1,2} & \cdots & M_{1,N} & \cdots & M_{1,N+7} & \cdots & M_{1,2N} \\ \vdots & \vdots & \ddots & \vdots & \ddots & \vdots & \ddots & \vdots \\ M_{10,1} & M_{10,2} & \cdots & M_{10,N} & \cdots & M_{10,N+7} & \cdots & M_{10,2N} \\ 1 & 0 & \cdots & 0 & \cdots & 1 & \cdots & 0 \\ M_{12,1} & M_{12,2} & \cdots & M_{12,N} & \cdots & M_{12,N+7} & \cdots & M_{12,2N} \\ \vdots & \vdots & \ddots & \vdots & \ddots & \vdots & \ddots & \vdots \end{bmatrix} \begin{bmatrix} \boldsymbol{V}_{1,1} \\ \boldsymbol{V}_{1,2} \\ \vdots \\ \boldsymbol{V}_{1,N} \\ \boldsymbol{V}_{2,1} \\ \vdots \\ \boldsymbol{V}_{2,7} \\ \vdots \\ \boldsymbol{V}_{2,N} \end{bmatrix}$$

FIGURE 4 (A) Correlated pixels and (B) mapping matrix for image generation and the $N+7$th columns, representing the pixel locations to be added in two virtual panels. In this way, all the elements in mapping matrix M can be found. For a desired high-resolution image, each pixel value is factorized into two pixel values, which consists of two low-resolution images respectively, according to Equation 1. Then, the luminance separation ratio for each pixel can be obtained by comparing the pixel values of two virtual panels. Meanwhile, the total luminance of each pixel in the display panel can be calculated by adding the corresponding two pixel values of two virtual panels.

In our proposed system as shown in Figure 5, PR and QWP are the components that control the luminance separation ratio for each pixel. PR is a device that can adjust the orientation angle of a linearly polarized light for each pixel so that the ratio of TE and TM components can be adjusted. With the help of QWP, the TE and TM linearly polarized lights are converted to RCP and LCP, respectively. Therefore, when PR adjusting the ratio of TE and TM components, the PML is adjusting the ratio of RCP and LCP, which is the polarization eigenstates of PBD. In the experiment, a twisted-nematic (TN) LC panel is adopted to work as the PR. The top polarizer of the TN LCD panel is removed. By adjusting the voltage of the cell, the ratio between TE and TM components can be adjusted even though there might be a phase difference between TE and TM components.

2.2 | Imaging results

To test the performance of the proposed system, a resolution target "Siemens star" is used. The imaging results are shown in Figure 6. Comparing the original picture (Figure 6A) with the resolution-enhanced picture (Figure 6B), the screen-door effect is apparently reduced. The grating period of PBD in the system is much longer than the visible wavelength so that the diffraction angle of PBD is very small and chromatic dispersion is negligible. On the other hand, the diffraction angle of PBD will vary as the incident angle changes, but this difference can be decreased by image rendering process and eyepiece lens digital aberration correction.

3 | BROADBAND WIDE-VIEW PBD

3.1 | PBD structure design

In the proposed resolution enhancement method, PB phase gratings that can achieve high efficiency for broadband wavelength and large incident angle are desirable.[16] By taking the advantage of self-aligning property of LC, broadband retardation control with compact form factor based on multi-twist structure has been demonstrated.[17,18] Dual-twist achromatic PG shows a much broader bandwidth than the single-layer PG, and it can cover most of the visible range.[19] However, the angular response of dual-twist achromatic PG is even worse than that of single-layer nontwist PG.[20] In order to get achromatic wide-view PG, more degrees of freedom are needed. Therefore, we design a three-layer multi-twist grating structure, which can achieve high efficiency in the visible spectral region and at large incident angle. The rigorous coupled-wave analysis method was applied to simulate the three-layer multi-twist grating structure. The thicknesses d of the three layers are 0.9, 1.32, and 0.88 μm, and the corresponding twist angles ϕ are $-69.4°$, $3.7°$, and $64°$, respectively. Figure 7 shows the side view of the device structure.

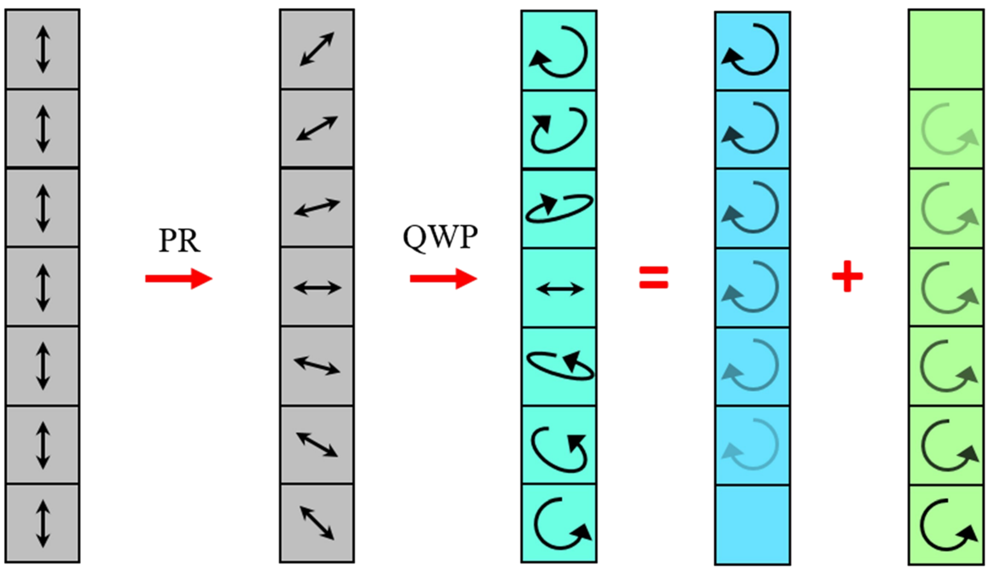

FIGURE 5 Illustration of polarization states through the PML. PML, polarization modulation layer; PR, polarization rotator; QWP, quarter-wave plate

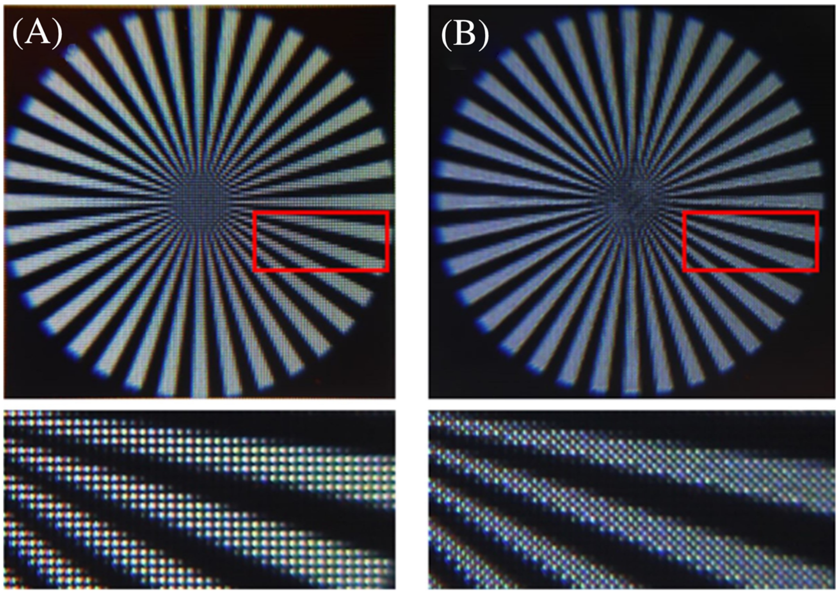

FIGURE 6 Captured images of (A) original and (B) enhanced resolution of a "Siemens star" resolution target

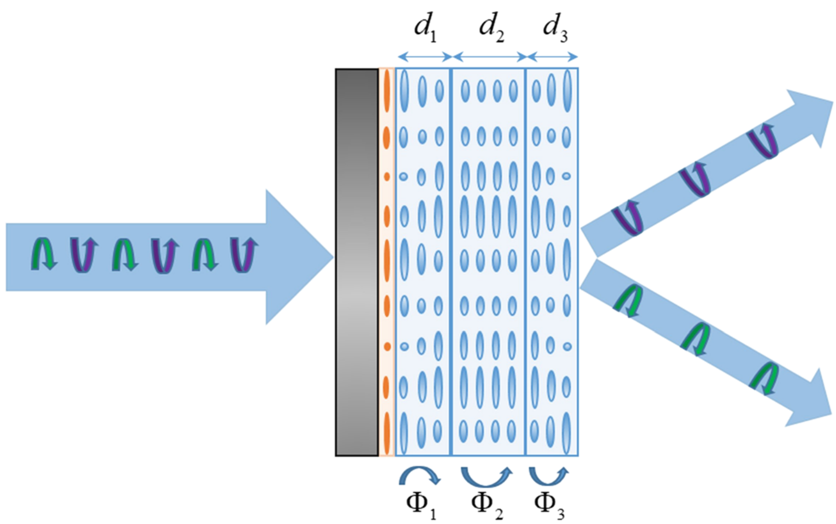

FIGURE 7 Structure of three-layer multi-twist PB phase grating. PB, Pancharatnam-Berry

3.2 | Device fabrication

In experiment, we fabricated a three-layer multi-twist PB phase grating. In order to form the grating pattern, photo-alignment method was adopted.[21, 22] A thin photo-alignment layer was spin coated on a glass substrate. The photo-alignment layer consists of brilliant yellow and dimethylformamide (DMF). After the spin-coating process, the alignment layer was exposed under the experimental setup (Figure 8). In the setup, a collimated beam ($\lambda = 457$ nm) is split into two orthogonal components by the first polarizing beam splitter (PBS). TM component transmits through the PBS, while TE component is reflected. The ratio between TE and TM components is adjusted by a half-wave plate (HWP), which is set after the laser source. The orientation of dielectric mirror M_3 can be adjusted to introduce linear phase difference between two optical paths along *x*-axis. The second PBS combines two beams and then makes the two optical paths merge together at the position where the substrate locates. Between the second PBS and substrate, there is a quarter wave plate (QWP), whose purpose is to convert the two linearly polarized beams to LCP and RCP, respectively. In order to get good pattern exposure, the intensity of LCP and RCP should remain the same at the front surface of the substrate. The photo-alignment layer was exposed to the laser output at ~15 mW/cm^2 for 20 minutes to get the designed grating pattern.

According to simulation, the targeted thickness of each layer is 0.9, 1.32, and 0.88 μm, and the corresponding twist angle is −69.4°, 3.7°, and 64°. In order to obtain these targeted values, we spin-coated three layers of reactive mesogen mixture (RMM) onto the substrate. After spin coating of each layer, UV photo-polymerization process was applied to form stabilized polymer film. The components in the RMM include

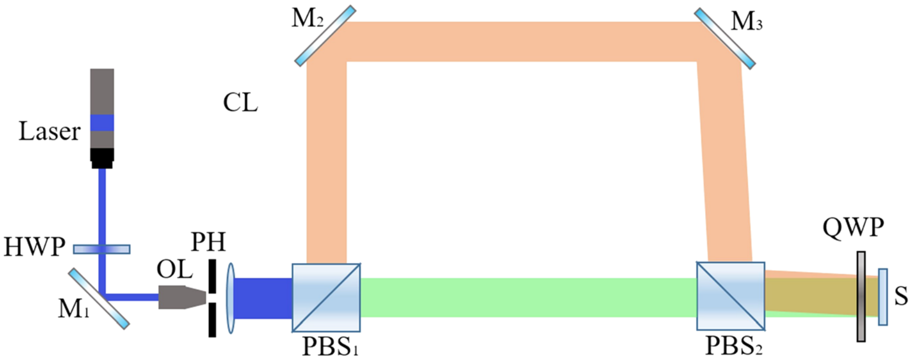

FIGURE 8 Experiment setup for polarization holographic recording of the PBD. PBD, Pancharatnam-Berry deflector

reactive mesogen RM257 (from LC Matter), photo-initiator Irgacure 651 (from BASF), surfactant Zonyl 8857A (from DuPont), and chiral S811/R811 (from HCCH). The chiral concentration in the first layer and third layer was 1.79% and 1.68%, respectively. For the second layer, because the twist angle was very small, and in experiment, we found that the LC molecules would not twist when the chiral concentration was too low. Therefore, we did not add chiral to the second layer so that the twist angle of the second layer was zero. This would bring negligible error for the efficiency performance according to the simulation.

3.3 | Imaging and testing results

The PB phase grating period was measured by a polarization microscope, and the result was around 35 μm. The PB phase grating was applied to image a keyboard, as Figure 9A shows. The output image from the PB phase grating is shown in Figure 9B, where the PBD sample is illuminated with the unpolarized ambient light. In Figure 9B, two ±1st-order diffracted lights are clearly observed in the output image. The zero-order leakage is negligible, which means the PB grating has nearly 100% diffraction efficiency in the visible spectral region. We can see a little yellowish color in the output image (circled area). It is because the alignment layer material has some absorption in the blue region.

The first-order diffraction efficiency of the PB phase grating was measured at three primary RGB wavelengths. Results are plotted in Figure 10A. At each wavelength, the angular spectrum was measured from −50° to 50° at 10° interval (Figure 10B-D). Experimental data agree well with simulation for the red and green lights; the average error is only ~2%. However, this error increases to ~5% for the blue light. A possible explanation is that blue light has a larger scattering.

4 | FURTHER DEVELOPMENT

In order to further increasing the image resolution, we can combine the time multiplexing (Figure 2A) and polarization multiplexing (Figure 3A). In our work, the original image is not observable; only shifted images are

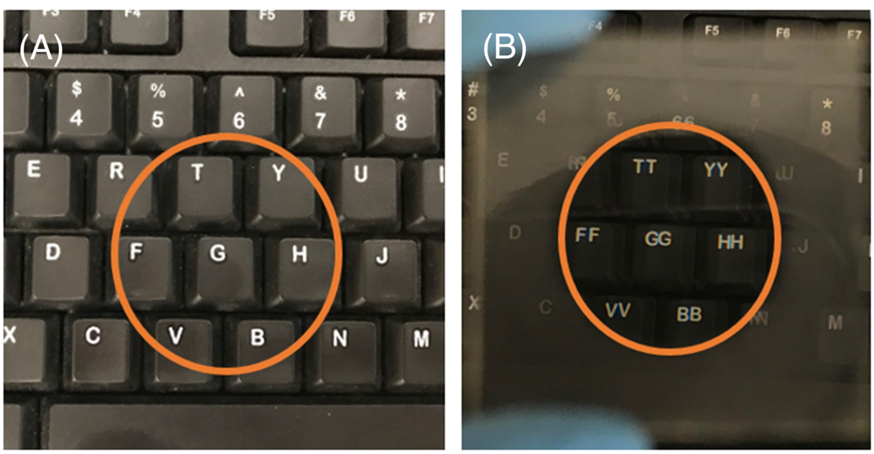

FIGURE 9 Broadband wide-view PBD imaging performance (A) input (B) output. PBD, Pancharatnam-Berry deflector

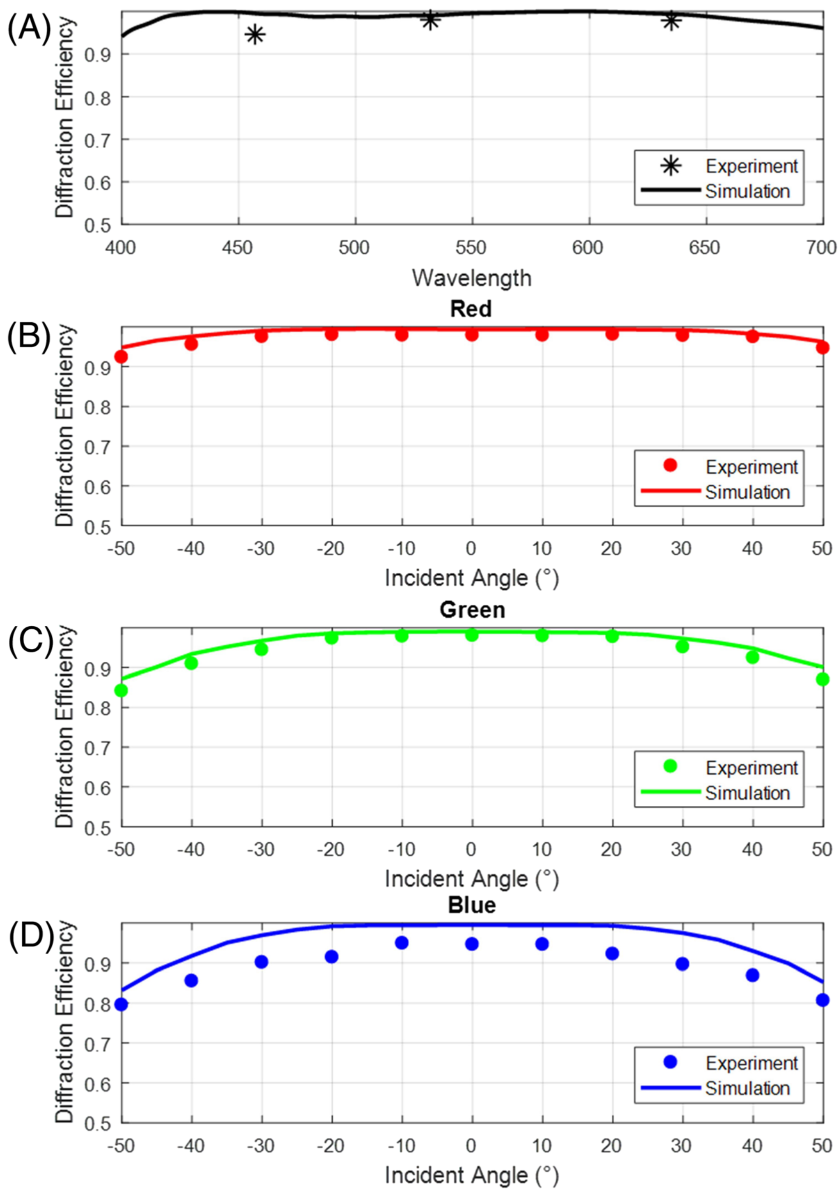

FIGURE 10 Simulated and measured (A) spectral and angular response of the fabricated PBD at (B) red, (C) green, and (D) blue wavelengths

present. By combining with the time multiplexing, the original image can exhibit and provide more information. The principle is illustrated in Figure 11. The original image and shifted images are present alternatively in time domain. The PBD should also change from passive addressing to active addressing. When the odd frames are

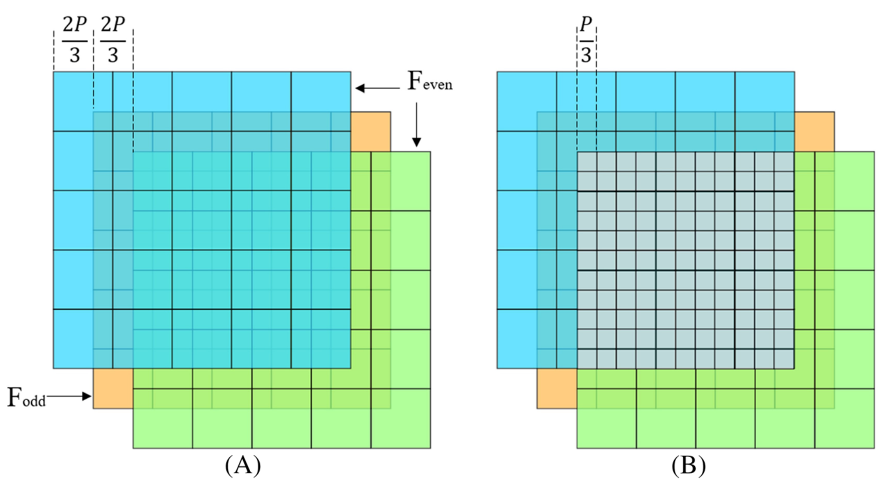

FIGURE 11 Operation principle of the shifted superimposition method to triple the resolution density. (A) The original panel (orange) presents at odd frames (F_{odd}), and the shifted panels (green and blue) present at even frames (F_{even}). (B) A new pixel grid (gray) with one third pixel pitch (P/3) is formed by superimposing three panels

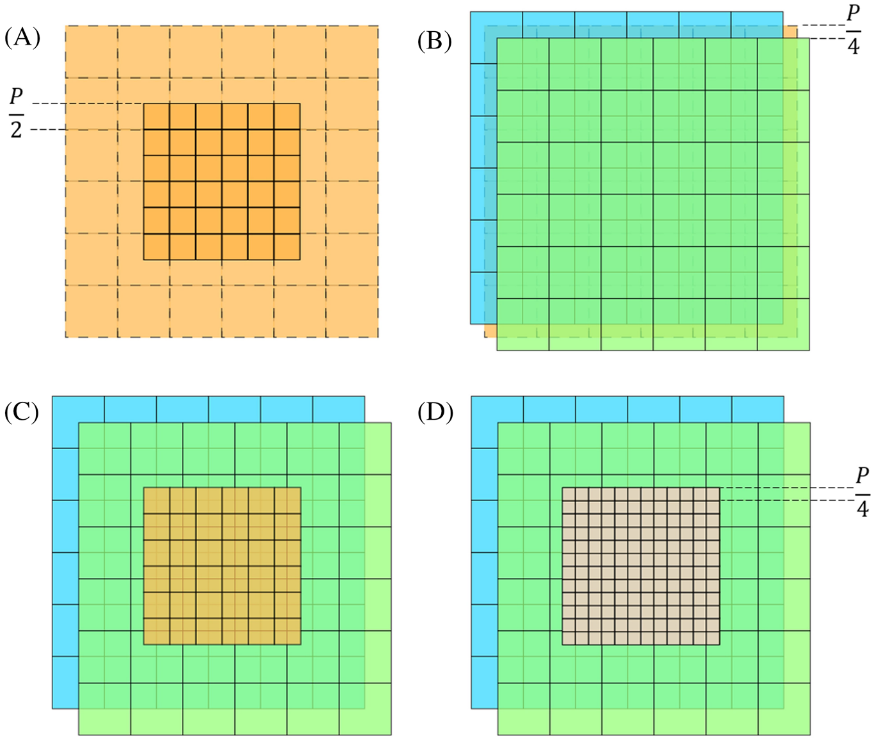

FIGURE 12 Operation principle of the shifted superimposition method to quadruple the resolution density in the fovea region. (A) The compressed panel (solid line orange) presents at odd frames (F_{odd}), and the shifted panels (green and blue) present at even frames (F_{even}). (B) A new pixel grid (gray) with quarter pixel pitch (P/4) in fovea region and half pixel pitch (P/2) in peripheral area is formed by superimposing three panels

on, the original image is exhibit, and the PBD will not deflect light. When the even frames are on, the PBD splits the original image and the shifted images appear. The deflection angle of PBD can be designed so that the deflected images can shift along opposite diagonal direction with $\left(2\sqrt{2}/3\right)P$. In this case, the overlap region of three images can triple the pixel density.

Moreover, the design of foveated display can be also combined with time multiplexing and polarization multiplexing. The key of feaveated display is generating high-resolution image in the fovea region. To achieve this goal, we can apply an active addressing PB lens to compress the original image to a small size optically so that high PPI image can be obtained in the fovea region. The operation principle is illustrated in Figure 12, whose difference with Figure 11 is that the compressed high PPI image is present at odd frames, rather than original image, and the shifting distance of the deflected image changes from $\left(2\sqrt{2}/3\right)$P to $\left(\sqrt{2}/4\right)$P. In fovea region, the PPI is four times to the original image and doubled in the peripheral area.

5 | CONCLUSION

We have demonstrated an optical method to improve the resolution of near-eye displays based on polarization multiplexing, with the help of a PBD and PML. The screen-door effect is significantly reduced. A high-efficiency broadband and wide-view PBD is also fabricated, whose spectrum and angular response agree with the simulation results very well.

ACKNOWLEDGMENTS

The authors are indebted to Intel Corporation and GoerTek Electronics for partial financial support and Guanjun Tan and Yun-Han Lee for useful discussion.

ORCID

Junyu Zou https://orcid.org/0000-0001-5218-3249
Jianghao Xiong https://orcid.org/0000-0002-8122-9936
Shin-Tson Wu https://orcid.org/0000-0002-0943-0440

REFERENCES

1. Cincotti G. Polarization gratings: design and applications. IEEE J Quantum Electron. 2003;39(12):1645–1652.
2. Packham C, et al. Polarization gratings: a novel polarimetric component for astronomical instruments. Publ. Astron. Soc. Pac. 2010;122(898):1471–1482.
3. Pancharatnam S. Achromatic combinations of birefringent plates. Part II. An achromatic quarter wave plate. Proc Ind Acad Sci. 1955;41(4):137–144.
4. Todorov T, Nikolova L, Tomova N. Polarization holography. 2: polarization holographic gratings in photoanisotropic materials with and without intrinsic birefringence. Appl Optics. 1984;23 (24):4588–4591.
5. Cheng HH, Bhowmik AK, Bos PJ. Concept for a transmissive, large angle, light steering device with high efficiency. Opt Lett. 2015;40(9):2080–2083.
6. De Sio L, Roberts DE, Liao Z, et al. Beam shaping diffractive wave plates [Invited]. Appl. Opt. 2018;57(1):118–121.

7. De Sio L, Roberts DE, Liao Z, et al. Digital polarization holography advancing geometrical phase optics. Opt. Express. 2016;24(16):18297–18306.
8. Lee YH, Zhan T, Wu S-T. Enhancing the resolution of a near-eye display with Pancharatnam–Berry phase deflector. Opt Lett. 2017;42(22):4732–4735.
9. Vieri C, et al. An 18 megapixel 4.3 ″1443 ppi 120 Hz OLED display for wide field of view high acuity head mounted displays. J Soc Inf Disp. 2018;26(5):314–324.
10. Tan G, et al. Foveated imaging for near-eye displays. Opt Express. 2018;26(19):25076–25085.
11. Osterberg G. Topography of the layer of rods and cones in the human retina. Acta Ophthal. 1935;6(Suppl):1–103.
12. Mitchell B. T., "Foveated display eye-tracking system and method," U.S. patent 7,872,635 (2011).
13. Allen W, Ulichney R. 47.4: Invited paper: Wobulation: doubling the addressed resolution of projection displays. SID Int Symp Dig Tech Pap. 2005;36(1):1514–1517.
14. Heide F, et al. Cascaded displays: spatiotemporal superresolution using offset pixel layers. ACM Trans. Graph. 2014;33(4):60.
15. Tan G, et al. Polarization-multiplexed multiplane display. Opt Lett. 2018;43(22):5651–5654.
16. Zou J, Zhan T, Xiong J, Wu S-T. Broadband wide-view Pancharatnam–Berry phase deflector. Opt Express. 2020;28(4):4921–4927.
17. Roberts D. et al., "Overcoming the tradeoff between efficiency and bandwidth for vector vortex waveplates," 2019 *IEEE Aerospace Conference*, Big Sky, MT, USA, (2019).
18. Komanduri RK, et al. Multi-twist retarders: broadband retardation control using self-aligning reactive liquid crystal layers. Opt Express. 2013;21(1):404–420.
19. Oh C, Escuti MJ. Achromatic diffraction from polarization gratings with high efficiency. Opt Lett. 2008;33(20):2287–2289.
20. Xiang X, Escuti MJ. Numerical modeling of polarization gratings by rigorous coupled wave analysis. Proc SPIE. 2016;9769:976918.
21. Schadt M, Schmitt K, Kozinkov V, Chigrinov V. Surface-induced parallel alignment of liquid crystals by linearly polymerized photopolymers. Jpn. J. Appl. Phys. 1992;31(Part 1):2155–2164.
22. Zhan T, Xiong J, Lee Y-H, Chen R, Wu S-T. Fabrication of Pancharatnam-Berry phase optical elements with highly stable polarization holography. Opt Express. 2019;27(3):2632–2642.

AUTHOR BIOGRAPHIES

Junyu Zou received his BS degree in Optical Information Science & Technology from Beijing Institute of Technology University in 2016 and MS degree in Optics and Photonics from University of Michigan-Ann Arbor in 2018. He is currently working toward a PhD degree from the College of Optics and Photonics, University of Central Florida. His current research interests include novel liquid crystal devices and near-eye displays.

Tao Zhan received his BS degree in Physics from Nanjing University in 2016 and is currently working toward a PhD degree from the College of Optics and Photonics, University of Central Florida. His current research interests include display system design, liquid crystal optical elements, and computational diffractive optics.

Jianghao Xiong received his BS degree in Physics from the University of Science and Technology of China (USTC) in 2017 and is currently working toward a PhD degree from the College of Optics and Photonics University of Central Florida, Orlando. His current research interests include near-eye displays and novel liquid crystal display devices.

Shin-Tson Wu is Pegasus Professor at the College of Optics and Photonics, University of Central Florida. He is among the first six inductees of the Florida Inventors Hall of Fame (2014) and a Charter Fellow of the National Academy of Inventors (2012). He is a Fellow of the IEEE, OSA, SID, and SPIE and an honorary Professor at Nanjing University (2013) and at National Chiao Tung University (2018). He is the recipient of 2014 OSA Esther Hoffman Beller Medal, 2011 SID Slottow-Owaki Prize, 2010 OSA Joseph Fraunhofer Award, 2008 SPIE G. G. Stokes Award, and 2008 SID Jan Rajchman Prize. Presently, he is serving as SID honors and awards committee chair.

How to cite this article: Zou J, Zhan T, Xiong J, Wu S-T. Increasing the pixel density for VR displays with a polarization grating. *J Soc Inf Display*. 2020;28:315–323. https://doi.org/10.1002/jsid.880